Evaluation of Explosion Scenarios

Development of Rule Based Analysis Method and Application to ¼-Scale and Full-Scale Simulations

Combustion Dynamics Ltd
Report CDL-1010

9 June 2000

Revised 3 September 2000

1. Introduction

The explosion investigation team for the TWA 800 accident was tasked to use available accident information and modelling tools to determine the most probable ignition location in the Center Wing Tank (CWT). This task required a review of the NTSB investigation reports to determine the damages caused by the initial explosion in the CWT. The modelling activities included fuel-air explosion calculations to determine the pressure loading on the various CWT components, and structural response calculations to determine the pressure loading required for an observed damage. The explosion modelling relied on initial JET-A air concentrations and temperatures determined from NTSB flight tests. As illustrated in Figure 1, the results of these activities were integrated into a rule-based scenario analysis which was specifically designed for this project to determine the level of consistency of different ignition locations with the observed damages.

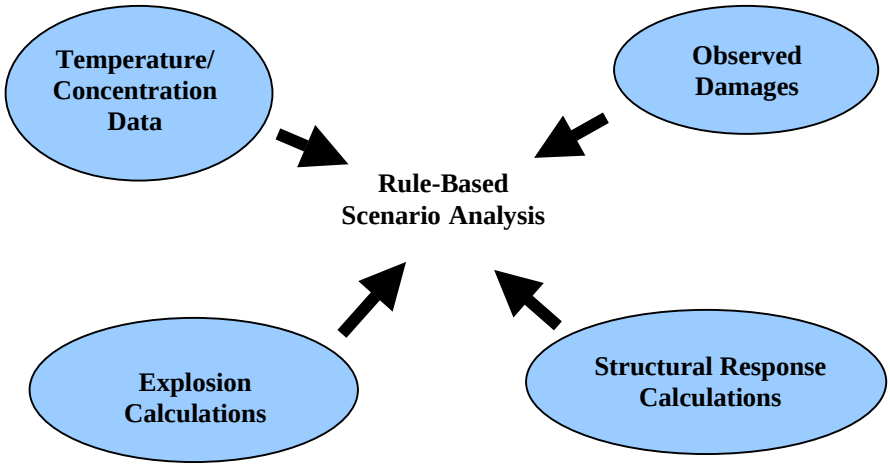

Figure 1: Integration of Accident Data and Modelling Calculations with Rule-Based Scenario Analysis to Determine Consistency of Different Ignition Locations with Observed Damages

2. Rule-Based Analysis Method

The objective of the rule-based analysis method is to provide a systematic approach to the analysis of a wide variety of data and calculations to determine an accident scenario that is consistent with observed damages. The main steps in the analysis are as follows:

1. ***Determine scenarios to be investigated.*** This step must be performed early in the analysis since it affects the observable damages that will be considered, and the types of calculations or experiments that should be performed. In the case of TWA 800, the scenarios involved a fuel-air explosion with different potential ignition locations.

2. ***Determine the observed damages that are relevant to the scenarios being considered***. In this step, it is equally important to identify components that were damaged and not damaged in the accident. Each selected damage (and non-damage) then becomes an "event" that forms the basis for a "rule" in the analysis.

3. ***Determine levels of confidence in the observed damages***. This very important step requires that the investigators assign a level of confidence for each "event". This addresses: 1) the level of confidence that the "event" actually occurred and 2) the level of certainty that the "event" is relevant to the scenario(s) being considered. In the case of the TWA 800 accident, the investigators were asked to provide levels of confidence that particular CWT components were damaged (or not damaged) in the initial explosion event. Levels of confidence may be assigned based on direct observation, and on calculations that indirectly assess the damage based on other observations. For the TWA 800 investigation, some structural elements were considered essential to the general wing integrity. The fact that this integrity was maintained during the initial explosion event indicated that these essential elements probably did not fail.

4. ***Compute the required structural loading for a particular event***. This step requires a structural response investigation of various components to determine the structural loading (or range of loading) that is consistent with a particular event (i.e. damage or non-damage). This investigation can be performed with experimental data or structural response analysis using simple engineering calculations or detailed finite element analysis. In this part of the analysis, it is also important to identify the loading parameters that are important for the structure being considered (e.g. peak pressure, impulse, pressure-impulse combination, tension-moment combination).

5. ***Compute the loading produced for the selected scenarios.*** Based on the relevant structural response parameters identified in Step 4, experimental data or computations are used to determine the loading for a particular scenario.

6. ***Provide uncertainties for Steps 4 and 5.*** As in the case of the observed damages, the loading and structural response calculations should be provided with levels of confidence which can be obtained from experimental statistical data or from subjective uncertainty estimates based on experience.

7. ***Integration of data into rule-based analysis.*** This step formulates the events identified in Step 2 into a set of rules. A probabilistic approach described in Section 3 is then used to compute a level of consistency of each scenario with each event. These consistency levels are then combined for an overall consistency with all events considered in the analysis.

Although the method described above was specifically designed for the TWA accident investigation, the approach could also be used to investigate any accident where various possible scenarios, or causes, must be evaluated in terms of their consistency with observed damages. In this sense, the terms "loading" and "damage" need not be restricted to structures since they could be extended to systems and personnel.

3. Probabilistic Approach Used in Rule Based Method

3.1 Definition of Probabilities

The rule-based method uses a probability approach to establish levels of consistency between accident scenarios and observed events which usually correspond to damage (or non-damage) of a structural component.

3.1.1 Probability of observable events

The events identified in Step 2 of the rule-based procedure are first numbered *i = 1, ...n*. Based on Step 3, the occurrence of an observable event, *i*, is assigned a probability $P_o(i)$ which increases from 0 to 1 with increasing level of confidence in the event. More specifically, a value $P_o(i) = 1$ indicates that the investigators are certain that the event occurred and that it is relevant to the scenario, whereas a value $P_o(i) = 0$ indicates that the event certainly did not occur or is not relevant to the scenario.

3.1.2 Probability of event for given loading conditions

Based on the structural response analysis, the probability, P_s, that an event, *i*, occurred depends on the values of the selected loading parameters, L_j, where $j = 1,..m$. This is a conditional probability which can be expressed as:

$$P_s(i|\, L_1 \ldots L_m) = P_s(i|\, \vec{L})$$

In the case of TWA 800, $\vec{L}$ corresponded to the peak pressure differential across the structural component involved in event *i*.

3.1.3 Probability of loading given initial conditions

The next step is to determine the probability, $P_{\vec{L}}$, of a given loading for each selected scenario. Since the loading depends on the initial conditions, I_i, where $i = 1,\ldots N$ prior to the accident, this is also a conditional probability $P_s(\vec{L}, i|\, \vec{I})$. For the TWA 800 accident, the main initial condition of interest involved the initial vapour temperature, T_o,

in the fuel tank. This temperature determined the initial fuel-air concentration prior to the explosion.

Knowing the probability density, $P_I(\vec{I})$, for the initial conditions, the probability that a particular loading, $\vec{L}$, occurred for an event, i, is given by:

$$P_L(L,i) = \int \ldots \int P_L(\vec{L},i|\vec{I})\, P_I(\vec{I})\, dI_1 \ldots dI_N$$

3.1.4 Probability of event based on structural response and loading analyses

Based on the structural response and loading calculations, the probability that an event occurred can now be expressed by considering all possible loadings so that:

$$P_c(i) = \int \ldots \int P_S(i|\vec{L}) P_L(\vec{L},i)\, dL_1 \ldots dL_m$$

3.2 Definition of Consistency Factors

The observed and computed probabilities, $P_o(i)$ and $P_c(i)$, provide the basis for determining the consistency of a scenario with observed damages. This can be done by defining consistency factors:

$$C_o(i) = 2\left[P_o(i) - 0.5\right]$$

$$C_c(i) = 2\left[P_c(i) - 0.5\right]$$

The consistency, $C(i)$, of a particular scenario with observation for event i is then expressed as the product:

$$C(i) = C_o(i) C_c(i)$$

such that $C(i) = 1$ and $C(i) = -1$ represent the limits where the scenario and observed damage are perfectly consistent and inconsistent, respectively.

Taking into account all considered events, a total consistency factor can then be defined as:

$$C_T = \sum_{i=1}^{n} C(i)$$

Since the maximum possible total consistency factor is given by:

$$C_T(\max) = \sum_{i=1}^{n} \left| C_o(i) \right|$$

a normalized total consistency factor can then be defined as:

$$c_T = C_T / C_T(\max)$$

such that $C(i) = 1$ and $C(i) = -1$ represent the limits where the scenario is, respectively, perfectly consistent and inconsistent with all observed damages. The above definitions for C_T and c_T automatically assign more weight to events which the investigators, based on observed damages, have a high degree of confidence that the events did or did not occur. If the investigators are totally unsure, $P_o(i) \to 0.5$ and $C_o(i) \to 0$ for that event.

The rule-based analysis method described in this section is relatively general and can be applied to any investigation where the objective is to determine the consistency of selected scenarios with observed damages. It should be noted that the term "observed damages" may represent a direct observation or an inferred observation based on other damages. It should be emphasized, however, that the method is limited by the fact that it assumes that the various events or rules are independent. If the occurrence of an event, *i*, affects that of another event, *j*, the conditional probability, $P_c(i|j)$, must be calculated. This is the case, for example, for scenarios involving progressive damage where the failure of one component can affect the loading and damage of other components. Progressive failure scenarios are not addressed in this report and all events or rules are assumed to be independent.

4. Application of Rule-Based Method to TWA 800

4.1 Observed Damages, (P_o)

An initial list of observed damages, potentially relevant to the initial explosion event, was prepared by CDL based on the damage sequence analysis prepared by TWA 800 crash investigators [1]. This list was presented to Boeing and NTSB investigators at a meeting in Seattle to assign levels of confidence that these damages were indeed the result of the explosion in the CWT. This process was continued by Boeing personnel, who finalized the levels of confidence with supporting comments that were reviewed and supplemented by NTSB personnel. The main CWT components considered in the analysis included the Front Spar (FS), SWB3, SWB2, Mid Spar (MS), SWB1 and Rear Spar (RS). The failure of the manufacturing door on SWB2 and the deformation of the doors on SWB1 in the aft direction were also considered. The failure or integrity of the various beams were determined based on direct observations and on calculations related to the wing integrity during the initial explosion event. Based on these two approaches, a

combined confidence level was then determined. The final result of this exercise has been reported by Boeing and NTSB [2], and is included in Appendix 1.

The levels of confidence, $W_o(i)$, in the above analysis were classified according to the definitions in Table 1. Based on that classification, the probability, $P_o(i)$, was calculated as $P_o(i) = W_o(i)/100$, where $W_o(i)$ is based on the combination of directly observed "Inspection" and "Calculation" values listed in Appendix I . Taking into account damages or deformations in both forward and aft directions, the resulting probabilities, $P_o(i)$, were evaluated as listed in Table 2.

Evaluation of Event	$W_o(i)$
Almost Certainly Did Not Happen	0%
Low Probability of Happening	25%
Equal Probability of Happening	50%
Likely Happened	75%
Probably Happened	90%
Almost Certainly Happened	100%

Table 1: Classification of Events

Event Rule	Description	$P_o(i)$	Event Rule	Description	$P_o(i)$
1	FS fails forward	1	**12**	SWB1 (left) fails aft	.05
2	FS fails aft	0	**13**	SWB1 (right) fails forward	.05
3	SWB3 fails forward	1	**14**	SWB1 (right) fails aft	.05
4	SWB3 fails aft	0	**15**	RS (left) fails forward	0
5	SWB2 fails forward	.125	**16**	RS (left) fails aft	.25
6	SWB2 fails aft	.125	**17**	RS (right) fails forward	0
7	MS (left) fails forward	.05	**18**	RS (right) fails aft	.25
8	MS (left) fails aft	.05	**19**	SWB1 L. door deforms fwd.	0
9	MS (right) fails forward	.05	**20**	SWB1 L. door deforms aft	1
10	MS (right) fails aft	.05	**21**	SWB1 R. door deforms fwd.	0
11	SWB1 (left) fails forward	.05	**22**	SWB1 R. door deforms aft	1

Table 2: Observed Probabilities Based on Analysis in Appendix 1

4.2 Structural Response Probabilities, $P_s(i|L)$

Structural response calculations were performed by Boeing to determine the response frequency and failure pressure for the various beams in the CWT, and the pressure differential required to produce the observed deformation of the SWB1 doors in

the aft direction. The frequency analysis indicated that the response frequency of the beams ranged between 90 and 240 Hz, corresponding to periods of 4 .2 - 11 ms [3]. These time scales are typically an order of magnitude shorter than the pressure loading time scales calculated by the explosion models or estimated by multiplying the 1/4 scale experimental time scales by the scaling factor of 4. Based on these results, it was concluded that the CWT structural components considered in Table 2 were responding statically to the pressure differential across them. Tables 3 and 4 list the estimated pressure differentials required to fail the various beams and to produce the observed deformations on the SWB1 doors in the aft direction. This data was provided by Boeing [4] with comments on the methods and assumptions used in the analysis (Appendix 2).

The "minimum" pressure column in Table 3 corresponds to "the "*Minimum initial failure strength*" typically determined by conventional stress analysis methods used in commercial airplane design for insuring that minimum strength will always exceed regulatory requirement." [4] The "maximum" pressure column corresponds to "the "*Estimated maximum initial failure strength*" typically determined from large finite element models capable of load redistribution in plastic range. Initial failure is determined by input % strain at failure." [4]. In addition to the assumptions given in Appendix 2, it should be emphasized that the failure pressures given in Table 3 do not account for progressive failure where the failure pressure for a beam may be decreased due to failure or damage of a neighbouring beam.

Based on this data, the probability functions were defined in terms of the loading pressure differential, ΔP. For the beams, a linear ramp function (Figure 3a) was assumed with $P_s(i|\Delta P) = 0$ for ΔP less than the minimum pressure in Table 1, and $P_s(i|\Delta P) = 1$ for ΔP greater than the upper-bound value in the "maximum" column. For the doors (Figure 3b), $P_s(i|\Delta P) = 1$ if ΔP falls in the range listed in Table 4 and is set to 0 otherwise.

	Minimum (psi)	**Maximum (psi)**
Front Spar	20	25-30
SWB3	20	25
SWB2	20	30-35
Mid Spar	20	35-40
SWB1	25	45-50
Rear Spar	30	45-50

Table 3: Failure pressures for CWT beams [4].

	Pressure (psi)
Left Door	45-55
Right Door	20-25

Table 4: Pressure Differentials Required for observed deformations of SWB1 doors in aft direction [4].

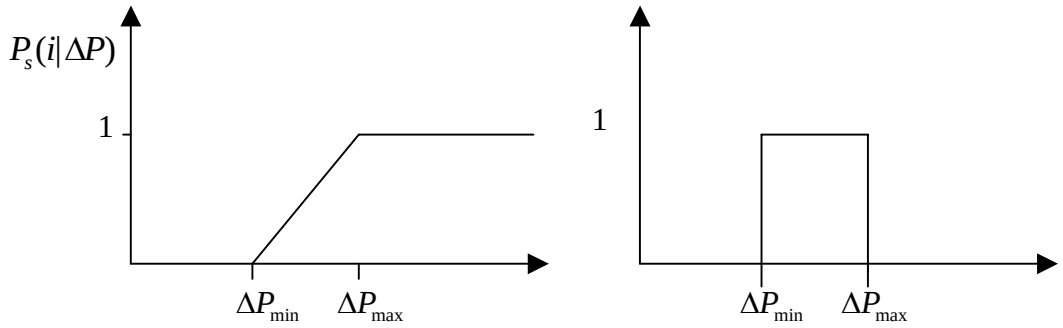

Figure 2: Structural Probability Functions $P_s(i|\Delta P)$ for CWT beams (left) and SWB1 doors (right).

4.3 Loading Calculations of P_L(L,i|I)

The remaining task is to calculate the loading probability function $P_L(\vec{L}, i|\vec{I})$. Due to the static response of the structure, and the modelling assumptions described in Section 4.2 and Appendix 2, the peak pressure differential, ΔP, was the only loading parameter, L, considered in this study. The initial condition of interest was mainly the initial bulk temperature, T_o, of the CWT ullage which, based on flight tests, was believed to be between 40°C and 50°C.

The peak pressure differentials across beams and doors were calculated using explosion modelling codes developed by Christian Michelsen Research (CMR) [5] and Sandia National Laboratories [6,7]. The probability, $P_L(\Delta P, i|T_o)$, could then be obtained by using the calculated values ΔP as the mean value in a Gaussian probability density function. The details of the CMR and Sandia models have been described in separate reports [5,6,7] that also outline the underlying assumptions and code validation with 1/4 scale experiments performed by Caltech, ARA and NTSB [8]. The CMR code, FLACS, calculates the 3-D flow field and flame propagation using a detailed Computational Fluid Dynamics (CFD) code based on the Reynolds Averaged Navier Stokes (RANS) equations. The Sandia code did not solve the detailed flow field but calculated the pressure differentials by combining a flame tracking model with global mass, momentum and energy conservation equations. The two codes complemented each other and were also used for code-to-code comparison. On one hand, the CMR code provided more details concerning the flow-field and could deal with scenarios involving progressive venting due to beam failure. On the other hand, the Sandia code's computational times

were orders of magnitude shorter than the CMR code. As discussed in the following section, both codes were useful in applying the rule-based analysis method to the TWA 800 investigation.

5.0 Application of Rule-Based Method

The main application of the rule-based method was to assess the consistency of different explosion scenarios with the observed damages. The scenarios involved different potential ignition locations identified by NTSB investigators. These locations, shown in Figure 3, corresponded to fuel probes (O), the compensator (C) and the terminator block (T).

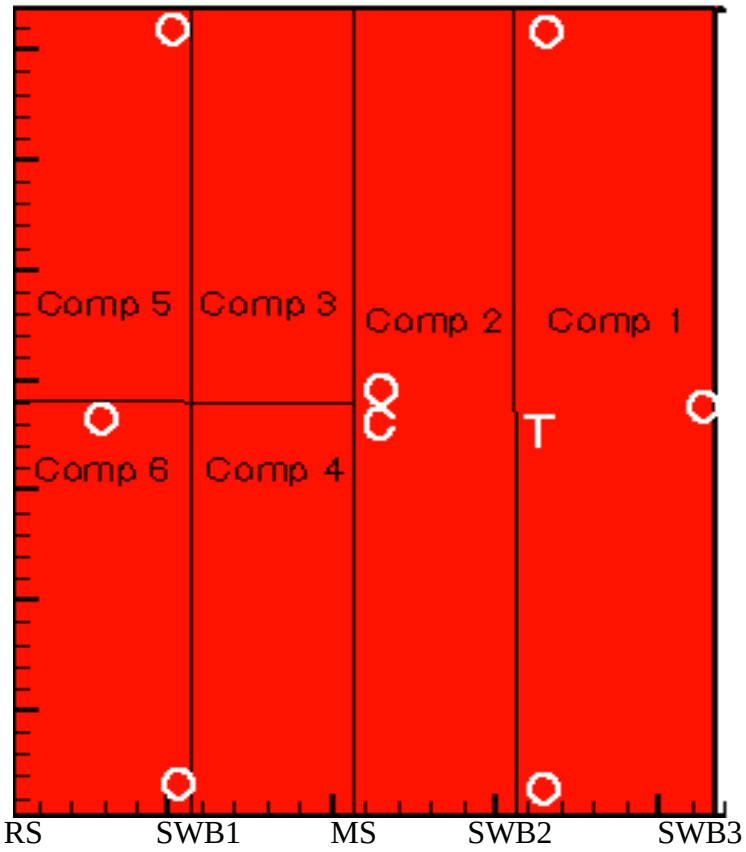

Figure 3: Top view of CWT where each compartment denotes a bay (front bay 0 not shown). Possible ignition locations considered in rule-based analysis: fuel probes (O), compensator (C) and terminator block (T).

The rule-based analysis method was used for two different types of applications: one involving the 1/4 scale apparatus with the simulant fuel and the other addressing the full-scale CWT geometry with Jet-A fuel.

5.1 Quarter Scale Geometry with Simulant Fuel

Following the quarter scale experiments with the simulant fuel, important questions were raised concerning the sensitivity of the pressure differentials to small changes in ignition location. This sensitivity was important in assessing the comparison between the explosion modelling code calculations and the 1/4 scale experiments. It also raised issues concerning the application of the codes to determine the ignition location in TWA 800. In order to investigate this effect, the Sandia code was used to compute the pressure differentials for three horizontal grids each containing 1850 evenly distributed ignition locations [6]. CMR code calculations were also performed for a coarser grid of locations in Compartment 2. These calculations were performed for the "all strong" configuration in the 1/4 scale experiments where all of the partitions were rigid.

The rule-based system used the Sandia results to 1) evaluate the sensitivity of the consistency factors to the ignition location and 2) determine if this sensitivity could be useful to determine more probable ignition locations for the full scale geometry. Referring to Table 2, rules 2, 4, 15 and 17 were excluded since these events were not possible for the geometry being considered. Rules 19 and 21 involving forward deformation of the SWB1 doors were also excluded since no structural response data was available for deformation of the doors in that direction. The results were presented in the form of contour plots where each position corresponds to a different ignition location, and the colour corresponds to the peak pressure differential or consistency factor for that location.

Figure 4 provides an illustrative example of relating pressure differentials computed with the Sandia code to the consistency factors computed with the rule-based system. The two figures are for Rule 5 involving failure of SWB2 in the forward direction. The pressure plot (left) indicates that the highest forward peak pressure differential occurs when the ignition location is near the center-rear of the CWT. As can be seen from the consistency plot (right), this high pressure results in a consistency factor of -0.75 for the fuel probe in this area which, due to the uncertainty in the observed damage, is the lowest possible value for this rule. This would indicate that this particular ignition location is highly inconsistent with the observation that SWB2 most likely did not fail during the explosion event. On the other hand, locations in the two forward compartments display a consistency factor of 0.75, indicating that they are very consistent with this observation.

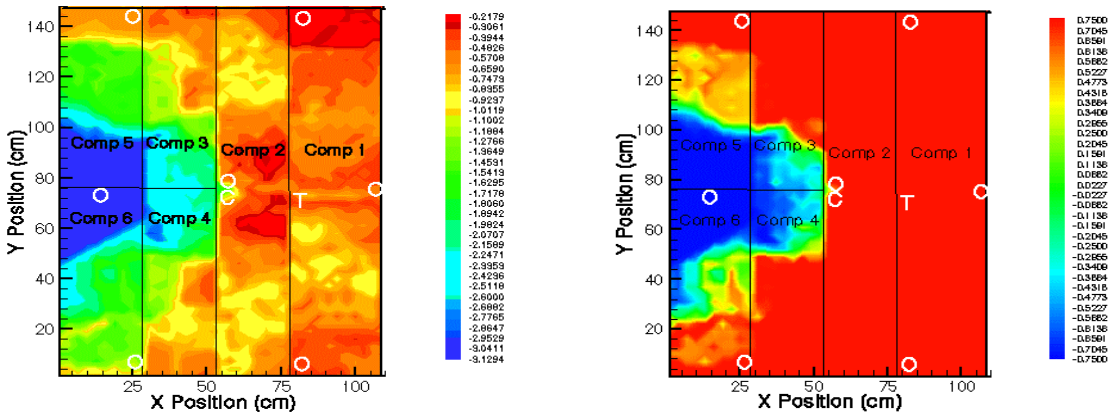

Figure 4: Contour plots displaying peak differential pressure (left) and consistency factor (right) as a function of ignition location for SWB2 failing in forward direction. Due to the sign convention used for the pressure differential, the highest peak pressure for this rule corresponds to the most negative value (i.e., blue region). The highest consistency factor corresponds to the red region.

Figure 5 displays the results for rules 8, 10 and 12 in Table 2, which correspond to failure of the Mid Spar (Left and Right) and SWB1 Left sections in the aft direction. The top two plots indicate that the highest peak pressure differentials and lowest consistency factors occur near the center of Compartment 1 where a fuel probe and a terminator block are located. The sharp asymmetry of these plots indicates that the consistency factor is very sensitive to which side of the center line the ignition is located. A similar sensitivity is observed for SWB1 Left, where the compensator ignition location in Compartment 2 and the fuel probe in Compartment 1 are located in regions with sharp gradients in peak pressure and consistency factor. This high sensitivity to ignition location is due to the complex geometry of the tank which includes a large number of holes. The flame path and pressure development is very sensitive to the relative position between the ignition location and neighbouring holes. This sensitivity must be kept in mind when interpreting the results of 1/4 scale experiments, explosion model predictions for the 1/4 and full scale CWT, and the rule-based assessment of potential ignition locations.

The normalized consistency factor displayed in Figure 6 (top) indicates that all positions have positive consistency factors. Since the normalized consistency factor is based on a sum for all the rules, a positive value indicates that the ignition location is consistent, on the average, with the rules for the observed damages (or non-damage). This does not imply, however, that the ignition location is consistent with every rule included in the analysis. In terms of the 9 potential ignition locations, the compensator and fuel probe in Compartment 2 fall in high consistency factor regions, whereas the fuel probe near the CWT center-line in Compartment 6 is in a region of relatively low consistency. As seen from Figure 6 (middle), the overall consistency of the various ignition locations increases significantly if the SWB1 door rules 21 and 22 in Table 2 are removed. This is due to the fact that the predicted pressure differentials across SWB1 in the aft direction were too

low to produce the observed aft deformations of the doors for most of the locations considered.

The consistency factors described in this section were calculated based on an uncertainty of 10% in the pressure loading predictions. The sensitivity of the results to this uncertainty was examined considering an uncertainty of 100% with the door rules eliminated (Figure 6, bottom). Comparing Figures 6 (middle and bottom), it can be seen that the higher loading pressure uncertainty results in slightly less variation between the minimum and maximum normalized consistency factors. Nevertheless, the consistency order for the 9 potential ignition locations remains essentially unchanged, with the compensator and fuel probe in Compartment 2 displaying the highest consistency with observed damages and the fuel probe near the center-line in Compartment 6 being the least consistent.

Two rules were highly inconsistent with the computed pressure differentials for most of the ignition locations. As shown in Figure 7, these involved the observed aft deformation of the left and right doors on SWB1. The reason for this is that the peak pressure differentials across SWB1 in the aft direction was usually much lower than that required for observed deformation (Table 4).

The above analysis has illustrated the application of the rule-based analysis to determine the consistency of various scenarios to observed damages. Although, the method has highlighted the two most probable ignition locations, it should be noted that the calculations are based on a 1/4 scale geometry with a simulant fuel. Furthermore, no beams were allowed to fail during the explosion modelling calculation, thereby neglecting the sudden venting of the CWT which is known to have occurred when SWB3 failed. These limitations are addressed in the next section where the full-scale geometry is considered, with venting, using the combustion characteristics of a Jet-A fuel-air mixture. Consequently the above illustrative examples with the 1/4 scale geometry with the simulant fuel are not intended to provide any specific conclusions concerning the most probable ignition location in the full scale geometry with Jet-A fuel.

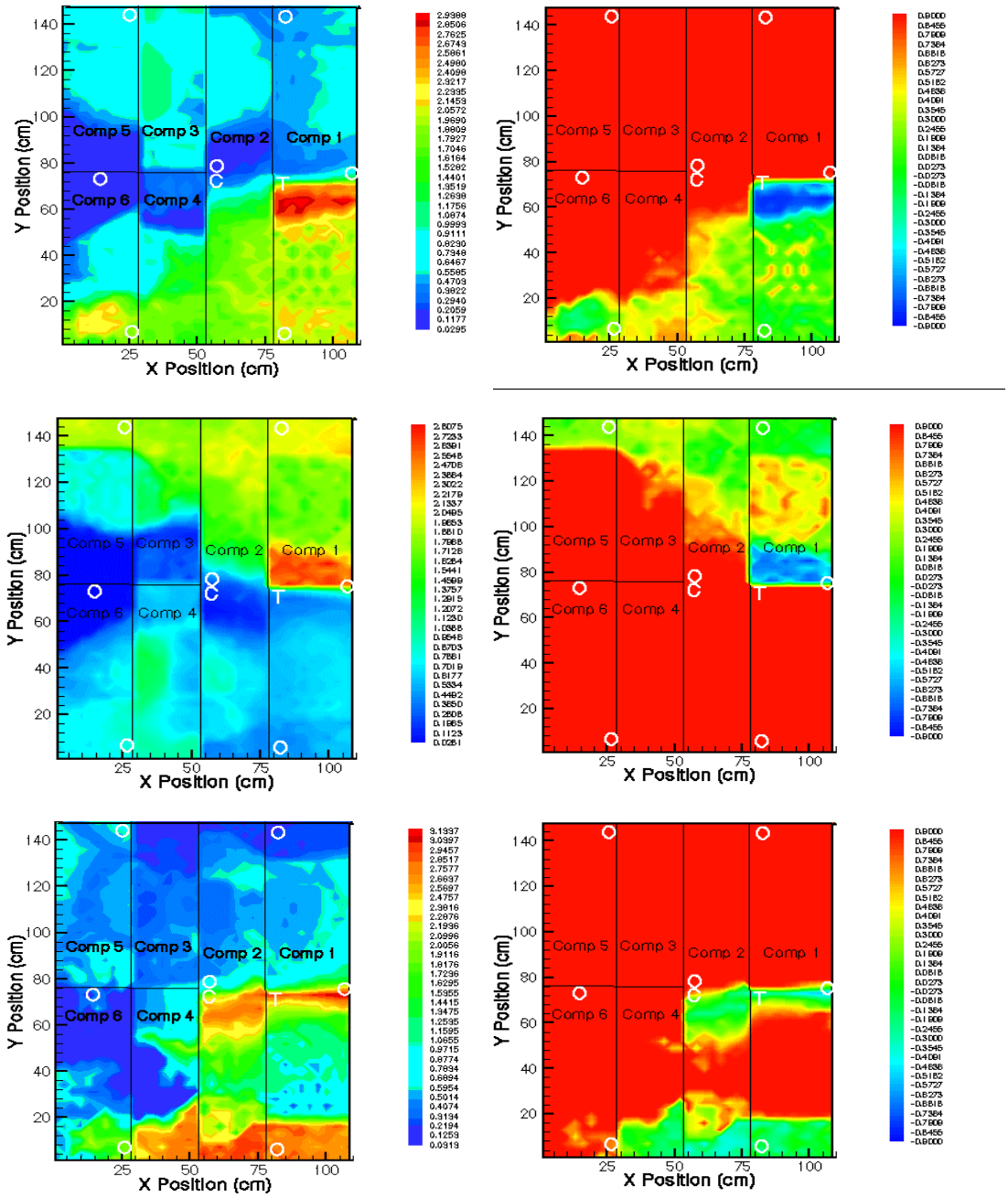

Figure 5: Contour plots displaying peak differential pressure (left plots) and consistency factor (right plots) as a function of ignition location for: 1) MS Left (top plots), 2) MS Left (middle plots), and 3) SWB1 Left (bottom plots). Due to the sign convention used for the pressure differential, the highest peak pressure for these rules corresponds to the most positive value (i.e., red region). The highest consistency factor corresponds to the red region.

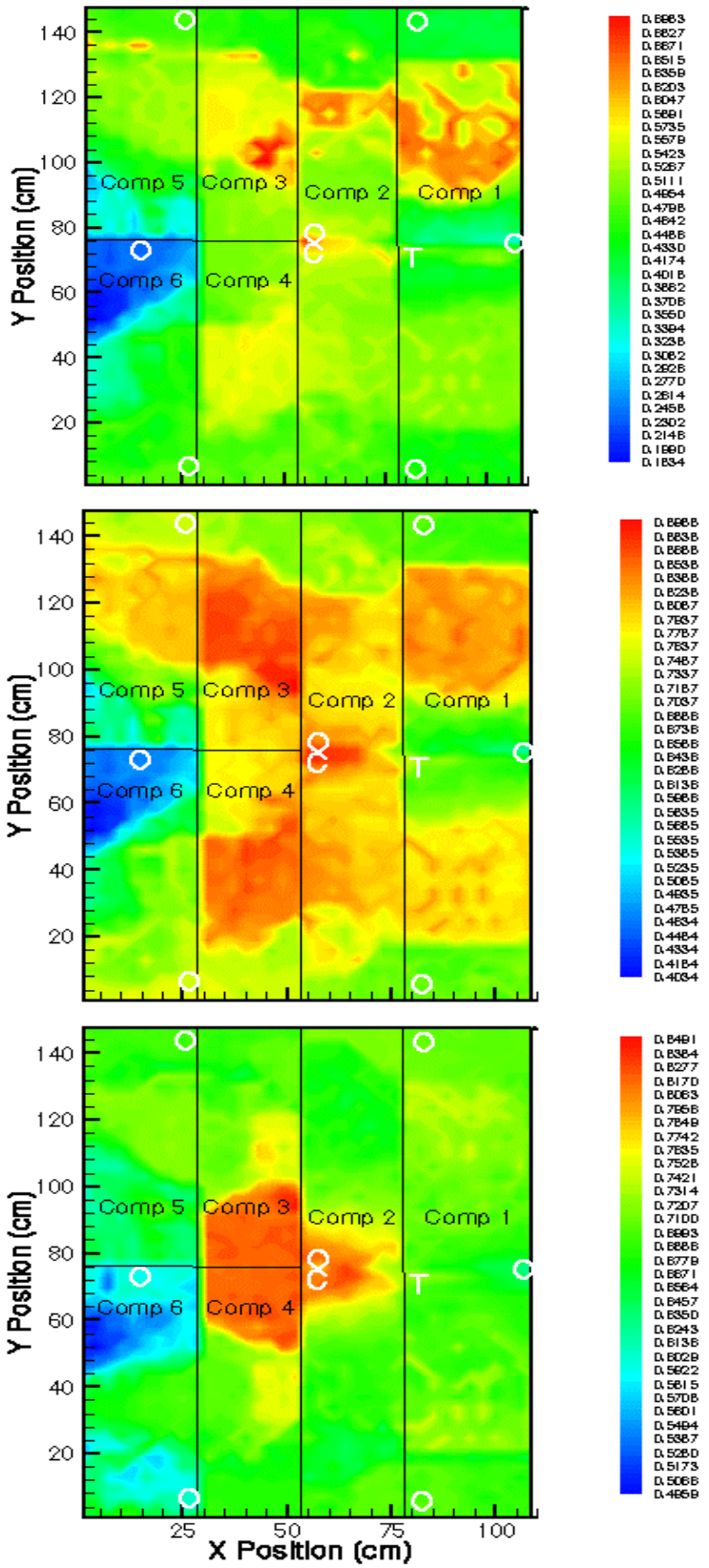

Figure 6: Normalized consistency factor. Top: SWB1 Door rules included, 10% loading model uncertainty; Middle: SWB1 Door rules excluded, 10% loading model uncertainty; Bottom: SWB1 doors excluded, 100% loading model uncertainty.

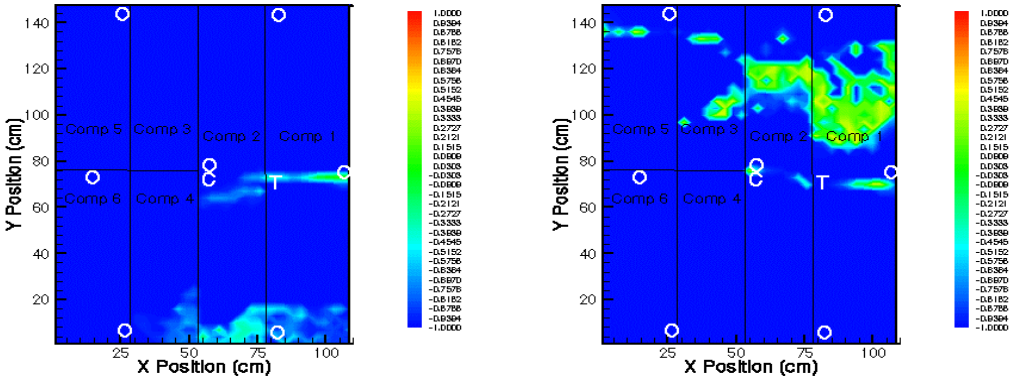

Left Door

Right Door

Figure 7: Consistency contour plots for SWB1 door deformation rules 20 and 22 in the aft direction.

5.2 Full-Scale Geometry with Jet-A fuel

The CMR and Sandia explosion modelling codes were used to model the full-scale CWT with a Jet-A fuel-air mixture. The full scale geometry differed from the 1/4 scale geometry not only in terms of its size but also in terms of the larger number of orifices in the structural members that divide the CWT into compartments. These orifices considerably increased the complexity of the flame propagation paths. The Jet-A fuel also introduced new modelling problems since experiments with Jet-A fuel in the 1/4 scale apparatus indicated that quenching often occurred when the flame attempted to propagate through an orifice. Based on a series of quenching experiments in the 1/4 scale apparatus, and data available in the open literature, the CMR and Sandia combustion models were extended to address the quenching phenomena. The details and limitations of these models are discussed in the CMR and Sandia reports [5,6,7] and in the project summary prepared by the fuel-air explosion investigation team [9].

In order to correctly model the explosion in the full scale geometry, it was important to recognize that the pressure development in the CWT was affected by the fact that SWB3 was known to have failed during the explosion. This failure also caused the subsequent failure of the Front Spar either through impact, and/or indirectly due to the resulting pressurization of the dry compartment. The sudden depressurization of the two forward compartments created a sudden pressure differential across SWB2. The magnitude of this pressure differential depended on a variety of factors including the rate of pressure rise behind SWB2 due to combustion, the rate of radiative heat losses, and the rate of venting through the small holes in SWB2. Based on initial venting calculations performed by CDL, it was determined that the time of failure of the SWB2 manufacturing door also played a role in determining the peak pressure differential across this beam. According to the sequence analysis and a structural analysis of the SWB2 door, it was determined that this door most likely failed due to the large loading on the keel beam. This loading occurred after the failure of the Front Spar and during the subsequent fracture propagation in the cargo bay. Based on coupled CFD-panel-motion calculations performed by CDL, it was estimated that the Front Spar was impacted by SWB3

approximately 16 ms after the failure of SWB3. This estimate, combined with an estimated ductile crack propagation speed in the cargo bay, indicated that the manufacturing door in SWB2 probably failed 16-40 ms after the failure of SWB3.

The above considerations were taken into account in a series of 32 CFD calculations performed by CMR. These calculations considered 8 potential ignition locations (Figure 8) and two initial vapour temperatures, 40°C and 50°C. The ignition locations corresponded to the 7 fuel probes and compensator probe locations. The analysis also considered two delay times, 16 ms and 40 ms, between the failure of SWB3 and the release of the SWB2 manufacturing door.

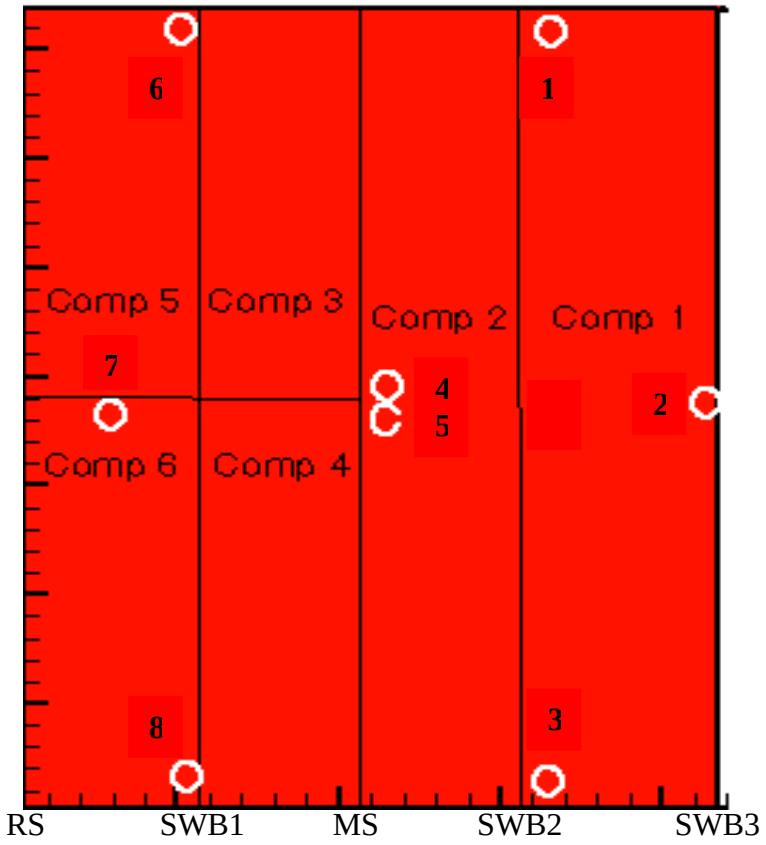

Figure 8: Eight ignition locations considered in CMR full scale calculations with Jet-A/Air mixture

The results provided by CMR included peak pressure differentials and combustion probabilities for the various compartments based on a quenching criteria for the connecting holes in the CWT. The peak pressure differentials in the CMR calculations were only used for partitions where combustion was complete on both sides of the partition. The pressure differential across a partition separating burned and quenched compartments was estimated based on the peak pressure in the burned compartment and the initial pressure in the unburned compartment. The pressure in the remaining compartments was estimated assuming isentropic expansion and compression of the burned and unburned gases, respectively.

Preliminary calculations using the entire range (minimum-maximum) of failure pressures in Table 3 indicated considerable internal damage in the CWT. The lower range in this table is typically determined by conventional stress analysis methods used for airplane design to always exceed regulatory requirements. Since this conservative value may be too low for the present analysis, the results presented below are based on the "Maximum" column in Table 3, which is based on detailed finite-element calculations.

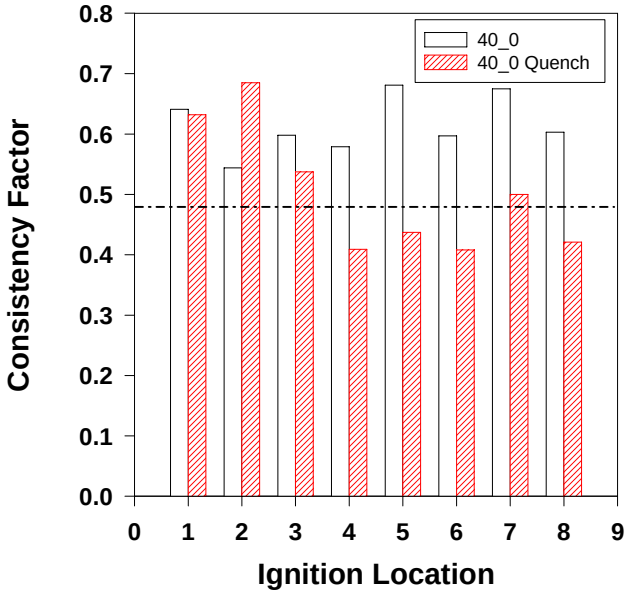

Figure 9: Consistency factors for 8 ignition locations neglecting and including quenching for Jet-A/Air at 40°C and 16 ms time delay for release of SWB2 manufacturing door after failure of SWB3. Dashed line indicates consistency factor if a uniform distribution between 0 and 2.75 bar is assumed for pressure differentials.

Figure 9 displays the normalized consistency factors for a 40°C initial temperature and a SWB2 manufacturing door release delay of 16 ms. Since only 8 ignition locations were considered for the full-scale geometry, the results are displayed as bar charts rather than the color contour plots used for the 1/4 scale analysis which considered 1850 possible ignition locations. The displayed results also compare the consistency factors including and neglecting quenching. It can be seen from this figure that the distinction between the ignition locations is much more evident when quenching is included. This is due to the fact that the quenching phenomenon is very sensitive to the ignition location and produces large pressure differentials at partitions between burned and quenched compartments. The dashed line in Figure 9 indicates the consistency factor (0.48) that would be calculated if, rather than using the detailed CMR calculations, a uniform distribution between 0 and 2.75 bar is assumed for pressure differentials. The maximum value of 2.75 bar corresponds to the peak pressure observed in single compartment experiments [10,11]. This line falls within the variation in consistency factor for different ignition locations, using the CMR calculations. It provides further indication that the

expected pressure differentials produced by a fuel-air explosion in the CWT result in a positive consistency factor with observed damages.

A more detailed view of the effect of quenching is provided in Figure 10, which displays the quenching pattern in the CMR calculations and the individual rule consistency factors for two ignition locations, 2 and 5. These locations were chosen due to their relatively high and low normalized consistency factors, respectively. It should be noted that the compartments in the CMR diagrams are plotted in the front-to-aft opposed to the aft-to-front direction in the previous Sandia plots for the 1/4 scale calculations. The CMR diagrams also include Compartment 0 (dry bay) which was not considered in the Sandia calculations. The green areas in the CMR diagrams indicate regions of complete combustion whereas the white areas indicate quenched regions. For ignition location 2, only one compartment is ignited resulting in sufficient pressure to fail SWB3, which is consistent with observed damages. However, the pressure differentials generated are insufficient to fail SWB2 and the other aft bays, which is also consistent with the observed damages. For ignition location 5, on the other hand, quenching occurs in compartment 1 and a large pressure differential is produced across SWB2 separating compartments 1 and 2. As seen from the two negative consistency factors, SWB3 does not fail whereas SWB2 fails; events which are inconsistent with observed damages. Finally, for both ignition locations, the pressure differential across SWB1 is insufficient to produce the observed deformation in the aft direction of the SWB1 doors. Consequently, this results in negative consistency factors for these rules.

Figure 11 (left) displays the normalized consistency factors for a 50^{o}C initial temperature, with and without quenching, and a 16 ms SWB2 manufacturing door release time. The dashed line in this figure indicates the consistency factor (0.32) that would be calculated if, rather than using the detailed CMR calculations, a uniform distribution between 0 and 3.5 bar is assumed for pressure differentials based on single compartment experimental data [10,11]. For a 50^{o}C initial temperature, very large differences in consistency factors are observed when quenching is included in the analysis. As seen in Figure 12, ignition location 2 remains very consistent with the observed damages for the same reasons previously given for the 40^{o}C calculations. Ignition locations 4 and 7 (Figure 13), on the other hand, display a low normalized consistency factor due to damages to internal beams and the insufficient pressure differential to fail SWB3. It should be noted that some of the regions in the CMR quenching diagrams display regions where the occurrence of quenching or complete combustion are not guaranteed due to the statistical nature of the quenching phenomenon. Also, for some regions, the flame quenching could not be determined due to the complexity of the flame paths. These regions are identified with a "?" in the diagrams. In the current analysis, quenching was assumed for regions with quenching probabilities larger than 50% and for regions with unknown quenching. It should be noted that no ignition location was found to satisfy all rules. This is due to the fact that the pressure differentials were not consistent with the observed deformations in the aft direction of the SWB1 doors.

The rule-based analysis method was also used to investigate the effect of various parameters on the normalized consistency factors for the 8 ignition locations. Figure 14 compares the consistency factors for delay times of 16 ms and 40 ms between the failure of SWB3 and the release of the SWB2 manufacturing door. A delayed release of the manufacturing door increases the peak pressure in Compartment 2 thereby increasing the pressure differential across SWB2 in the forward direction and across the Mid Spar in the aft direction. This results in a higher likelihood in failure of these beams which is inconsistent with the observed damages, and reduces the consistency factor. Finally, as seen in Figure 15, the normalized consistency factors depend on the uncertainty in the pressure loading calculations computed by the CFD code. The main effect of a higher uncertainty is to make the failure and non-failure of a beam more equally probable. This results smaller variations in normalized consistency factors between the various ignition locations as the uncertainty level is increased.

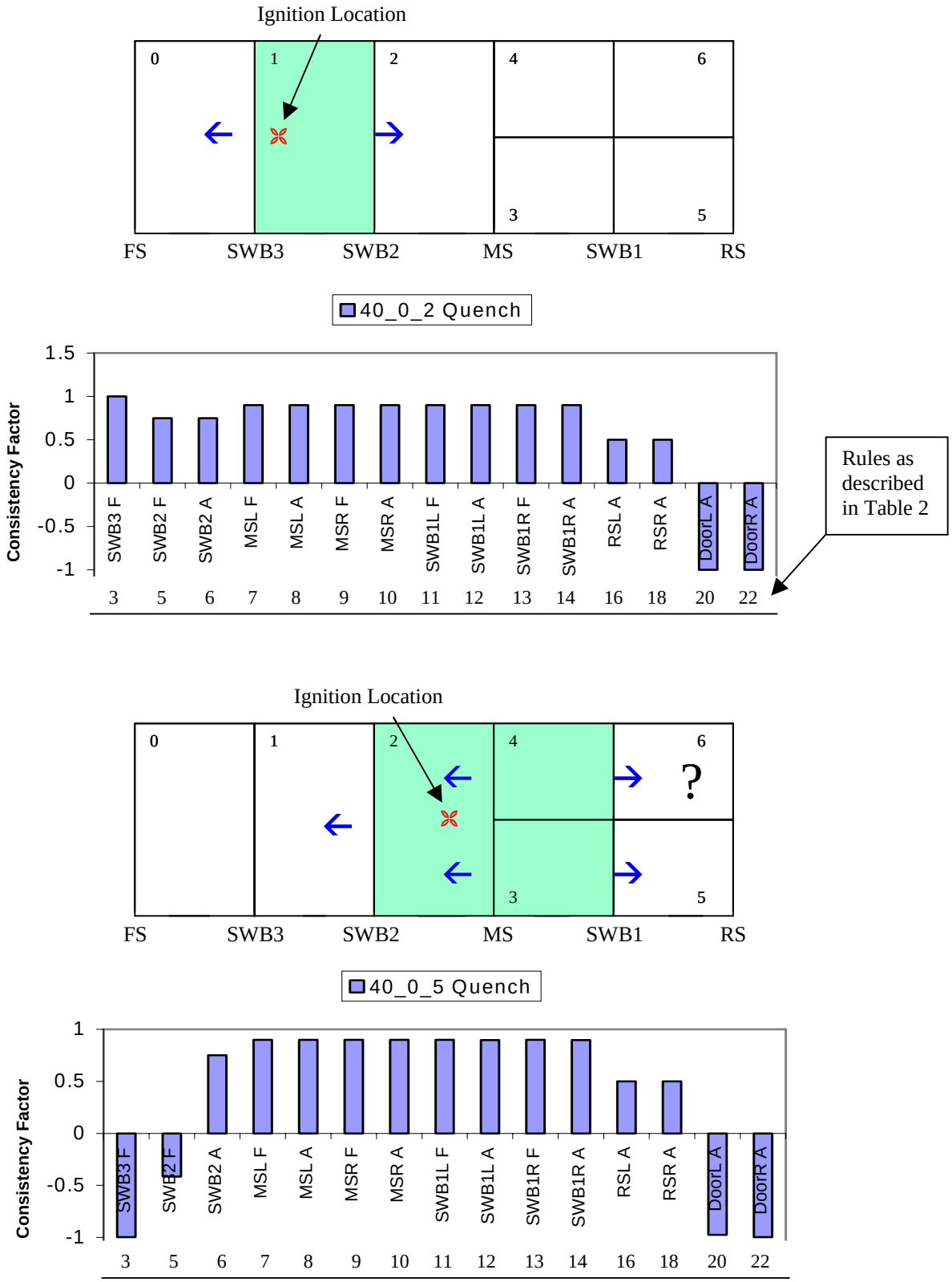

Figure 10: Quenching pattern and individual rule consistency factors for ignition locations 2 (top) and 5 (bottom). 40 ^{o}C initial temperature and 16 ms SWB2 release delay. Green and white areas in the quenching diagrams indicate fully burned and quenched regions, respectively.

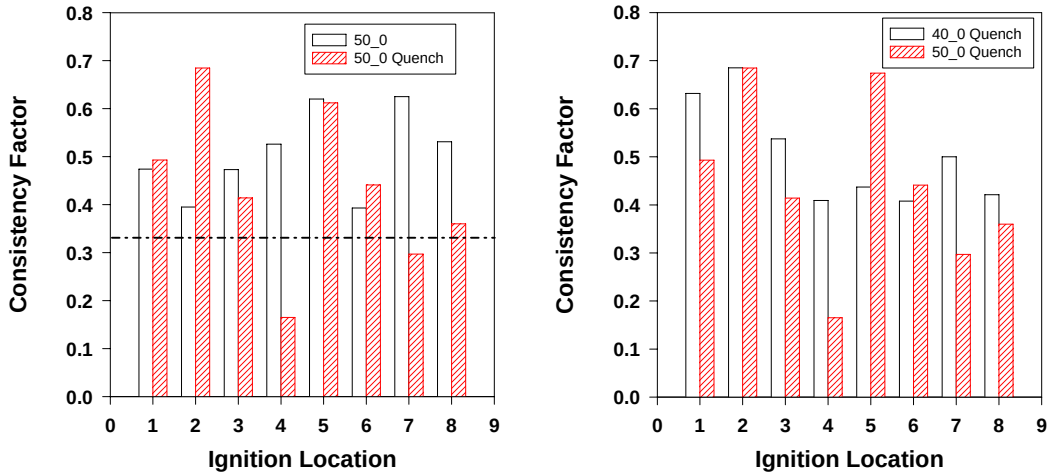

Figure 11: Left: Consistency factors for 8 ignition locations neglecting and including quenching for Jet-A/Air at 50°C; 16 ms time delay for release of manufacturing door after failure of SWB3. Dashed line indicates consistency factor if uniform distribution between 0 and 3.5 bar is assumed for pressure differentials. Right: Comparison of consistency factors for Jet-A/Air at 40°C and 50°C with quenching

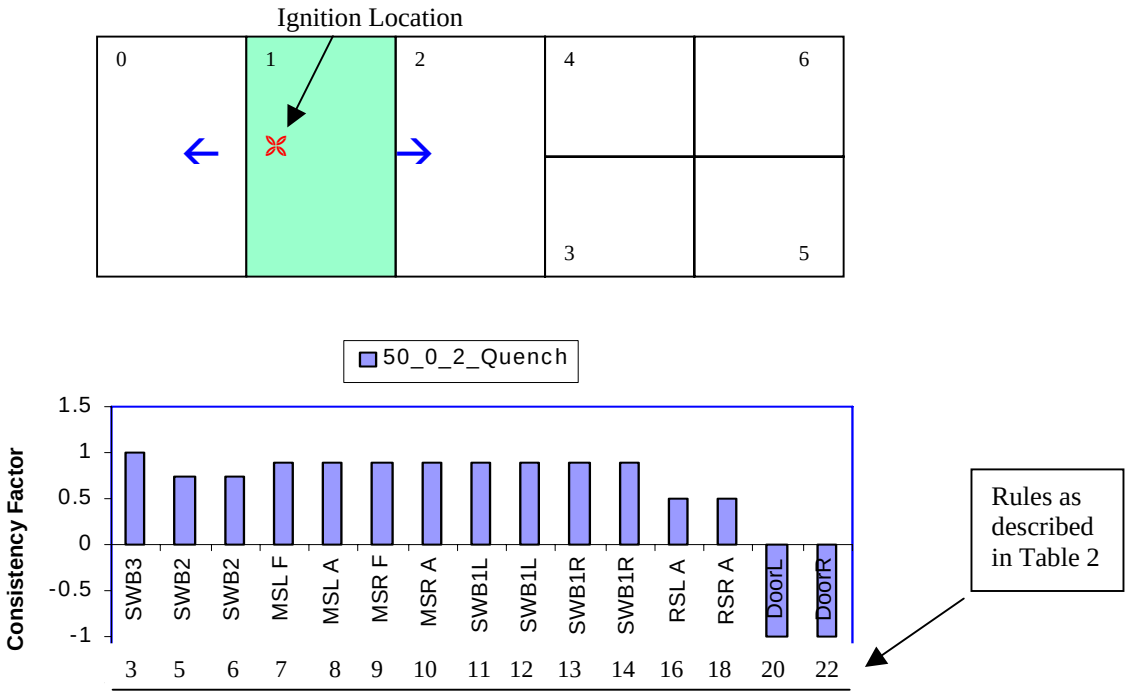

Figure 12: Quenching pattern and individual rule consistency factors for ignition location 2. 50°C initial temperature and 16 ms SWB2 release delay. Green and white areas in the quenching diagrams indicate fully burned and quenched regions, respectively.

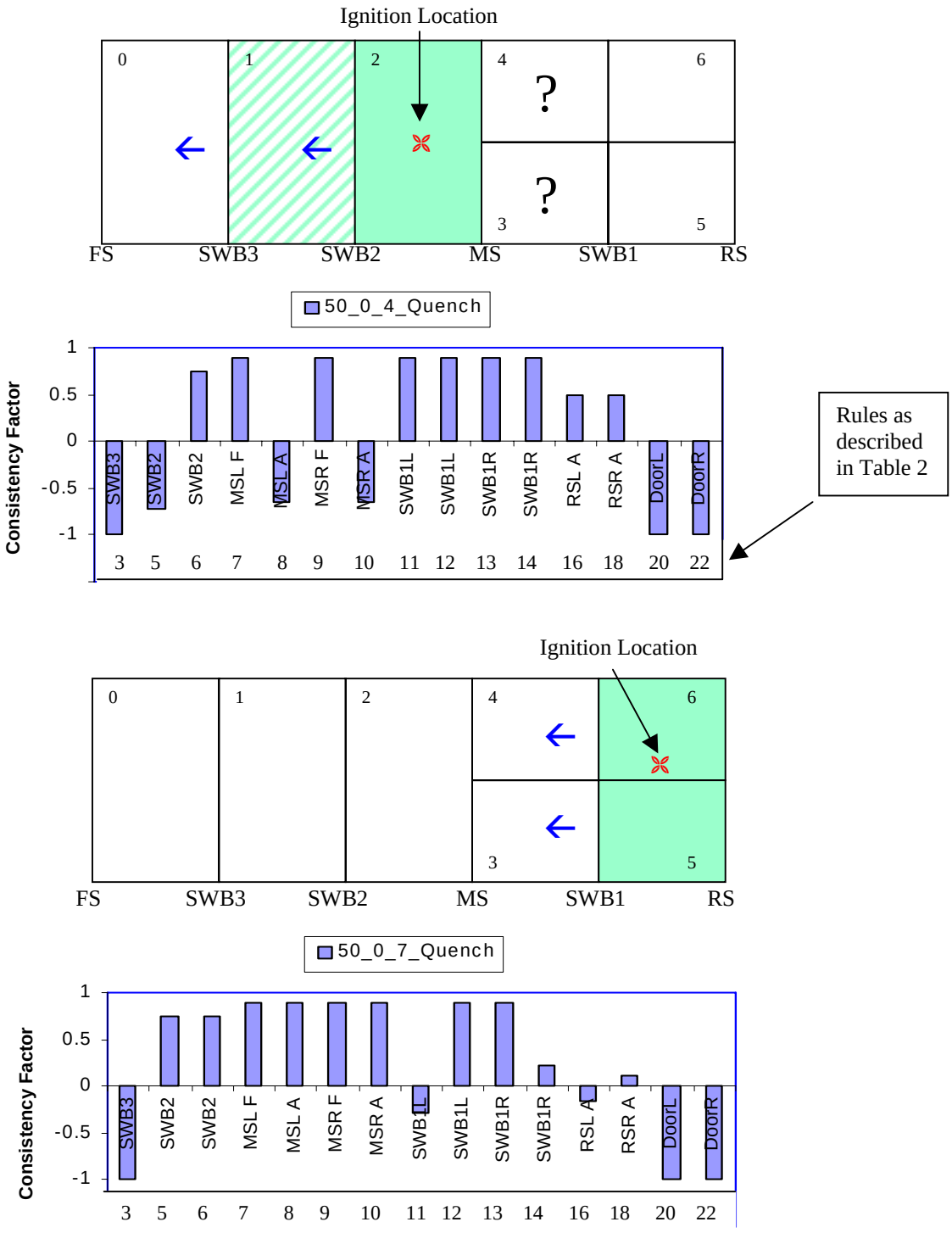

Figure 13: Quenching pattern and individual rule consistency factors for ignition locations 4 (top) and 7 (bottom). 50°C initial temperature and 16 ms SWB2 release delay. Green and white areas indicate fully burned and quenched regions, respectively. Cross-hatched areas indicate 64% probability of quenching.

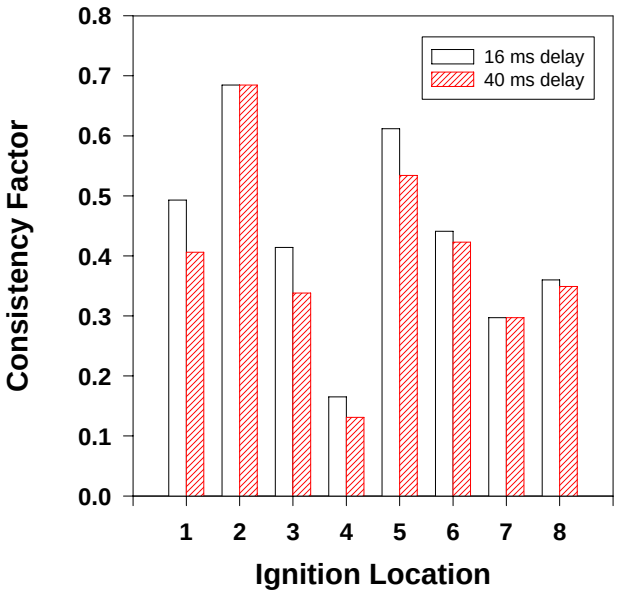

Figure 14: Comparison of normalized consistency factors for 16 ms and 40 ms delay between failure of SWB3 and release of SWB2 manufacturing door. Jet-A/Air at 50°C including quenching effect.

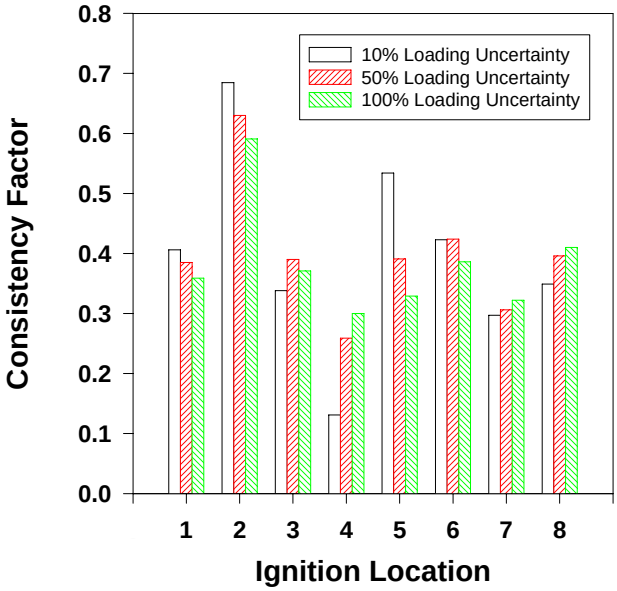

Figure 15: Comparison of normalized consistency factors with 10%, 50% and 100% pressure loading uncertainty from CFD calculations. Jet-A/Air at 50°C including quenching effect; 40 ms delay between failure of SWB3 and release of SWB2 manufacturing door.

6. Conclusions

This report presented a rule-based analysis method that can be used to assess the consistency of various scenarios with observed damages. The probabilistic approach requires the selection of scenarios, the determination of observed damages (or non-damage), and the use of pressure loading calculations and structural response criteria. The results are presented in the form of consistency factors which indicate the level of consistency of a particular scenario with the observed damages.

The rule-based analysis method was applied to the TWA 800 accident by using 1850 explosion modelling calculations performed by Sandia for the 1/4 scale geometry with simulant fuel and 32 calculations by CMR for the full-scale CWT with Jet-A fuel. The analysis for the 1/4 scale geometry indicated that the rule-based analysis method was a useful tool in distinguishing different ignition locations in terms of their consistency with the observed damages. Based on these results, the analysis was then applied to the full scale calculations performed by CMR for 8 potential ignition locations.

The main conclusions for the full-scale CWT geometry are as follows:

1. The overall "normalized" consistency factors were positive for all ignition locations considered in the analysis. This indicates that, on the average, the ignition locations were consistent with the observed damages.

2. The detailed CFD calculations indicate that the pressure differentials produced by an internal fuel-air explosion are consistent with the overall level of damage observed in the CWT. This conclusion is also supported by a simple uniformly random probability distribution analysis based on the peak pressures that were experimentally observed for Jet-A fuel-air mixtures between 40^{o}C and 50^{o}C. This simple analysis, which is not based on the CMR CFD calculations, indicates positive consistency factors of 0.48 and 0.32 for vapors at 40^{o}C and 50^{o}C respectively.

3. None of the ignition locations considered were consistent with all of the observed damages. In particular, the pressure differentials calculated by CMR were not consistent with the observed deformations in the aft direction of the SWB1 doors.

4. The most probable ignition location depends strongly on the initial temperature and on the quenching phenomena which are important for Jet-A/Air flames. Differences in normalized consistency factors between ignition locations are much more evident when quenching is present. This is due to the large pressure differentials created at a partition where quenching occurs.

5. The analysis indicates that the consistency factors for the eight ignition locations considered depends on the initial temperature in the CWT and the level of uncertainty in the in the CFD calculations. Much larger variations in the consistency factors were observed between the 8 ignition locations for a vapor temperature of 50^{o}C than for a

40^{o}C vapor when quenching was included in the CMR calculations. The distinction between the different ignition locations decreased, however, as the level of uncertainty in the CFD calculations increased.

6. The rule-based analysis also investigated the CMR calculations on the role of the delay time between the failure of SWB3 and the release of the SWB2 manufacturing door. A longer delay time resulted in a higher pressure differential across SWB2 and a lower consistency factor.

Although the analysis did reveal more probable ignition scenarios, a unique most probable ignition location could not be identified. This is due to a variety of reasons related to:

1. The uncertainties in extending the quenching models to the full scale geometry. This difficulty is compounded by the statistical nature of the quenching process which results in significant uncertainties in the actual flame propagation for a particular experiment or accident.

2. The high sensitivity of the flame propagation path to the small changes ignition location. This sensitivity was very apparent in the consistency factor contour plots discussed in Section 5.1 for the 1/4 geometry with the simulant fuel. It is also a factor for the full scale CWT with Jet-A due to the sensitivity of the quenching phenomenon to the distance between the ignition point and the nearest connecting orifice to an adjoining compartment.

3. The uncertainty in the initial fuel-air temperature, estimated from the flight data, which has a pronounced effect on the normalized consistency factors for the various ignition locations.

4. The uncertainties in the failure criteria for the CWT beams. It was particularly difficult to apply these criteria to an accident where complex progressive failure was involved. Also, it was not possible to validate the structural response criteria with experiments.

Although the method described above was specifically designed for the TWA 800 accident investigation, the approach could also be used to investigate any accident where various possible scenarios, or causes, must be evaluated in terms of their consistency with observed damages. In this sense, the terms "loading" and "damage" need not be restricted to structures since they could be extended to systems and personnel. The success of the method clearly depends on the uncertainties in the observed damages and in the calculations used to determine the loading and resulting damage. As formulated in this report, the probabilistic method is also restricted to cases where the observed damages can be formulated as independent events. This is clearly an assumption that may not be satisfied for accidents such as TWA 800 that typically involve complex damage sequences. Finally, the application of a probabilistic approach to accidents often requires

that uncertainties in the observed damages be estimated by crash investigators. For most practical situations, these estimates can only be made based on experience rather than on more reliable statistical data.

7. Acknowledgements

CDL would like to thank K. van Wingerden, J. Renoult, S. Armond of CMR and M. Baer and R.J. Gross of Sandia for providing the explosion calculations used as input in the rule-based analysis. The suggestions and contributions from J. Shepherd at CalTech, and J. Kolly and M. Birky at NTSB are also greatly appreciated. Finally the structural response data provided by Boeing and the contributions by Boeing and NTSB personnel to the observed damages list are also gratefully acknowledged.

8. References

1. "Metallurgy/Structural Group Chairman Factual Report Sequence Study" National Transportation Safety Board, Docket No. SA-516, Exhibit No. 18A, 1997.
2. Observed damages
3. S. Kari: "Response Spectrum Analysis", Boeing, October 1998.
4. "747-100 Wing Center Section Beam Overpressure Capability", Boeing, Jan. 1999.
5. K. van Wingerden, J. Renoult, S. Armond: "CFD Gas Explosion Simulations to Support the Investigation into the Cause of the Explosion in the Centre Wing Tank of TWA 800." Christian Michelsen Research Report CMR-00-30026, April 2000.
6. M.R. Baer and R.J. Gross (1998) A Combustion Model for the TWA 800 Center Wing Fuel Tank Explosion. Sandia National Laboratories Report SAND98-2043.,1998.
7. M.R. Baer and R.J. Gross: "Extended Modeling Studies of the TWA 800 Center-Wing Fuel Tank Explosion. Sandia National Laboratories Report 2000.
8. Shepherd, J. E., J. C. Krok, J. J. Lee, L. L. Brown, R. T. Lynch, T. M. Samaras, and M. M. Birky: "Results of 1/4-Scale Experiments, Vapor Simulant and Liquid Jet A tests." Explosion Dynamics Laboratory Report FM98-6, California Institute of Technology. 600 pp. , July, 1998.
9. M. Birky (NTSB), J. Kolly (NTSB), J. E. Shepherd (CIT), P. A. Thibault (CDL), M. R. Baer (SNL),K. van Wingerden (CMR), J. E. Woodrow (UNR), J. C. Sagebiel (DRI)"Summary and Conclusions of Explosion Research Team", 2000.
10. J. E. Shepherd, J. C. Krok, J. J. Lee, M. J. Kaneshige, L. L. Brown, R. T. Lynch, T. M. Samaras, J. Kolly, and M. M. Birky (2000). Results of ¼-Scale Testing: Simulant repeatability tests, Jet Avapor, and quenching. Explosion Dynamics Laboratory Report FM00-2, California Institute of Technology.
11. J. E. Shepherd, J. C. Krok, and J. J. Lee (1999) Spark Energy Measurements in Jet A. GALCIT, Report FM 97-9. Published May 3, 1999. 84 pp.

Appendix 1

List of Observed Damages

Appendix 2:

Table of Provided by Boeing for Beam Failure and SWB1 Door Deformation

747-100 Wing Center Section
Beam Overpressure Capability (updated Jan. 1999)

	Minimum Initial Failure Strength ✶ ✸ ✹ ❋ (psi)	Estimated Maximum Initial Failure Strength ✶ ✸ ✹ ⌖ (psi)
Front Spar	20	25-30
Spanwise Beam #3	20	25
Spanwise Beam #2	20	30-35
Midspar	20	35-40
Spanwise Beam #1 ⌖	25	45-50
Rearspar	30	45-50

✶ *Failure loading condition* assumed to be dominated by a bending moment in beam stiffeners (due to overpressure gradient across beam) as opposed to an axial load in beam/stiffeners (due to almost equal overpressure on both sides of beam). Expected failure generally in upper joint between stiffener and wing panel.

✸ *Initial failure level* shown but subsequent failures resulting in overall beam failure and venting generally expected to immediately follow (providing load gradient maintained)

✹ *Uncertainty range* intended to also envelope variation in capability for both forward acting pressure gradient and aft acting gradient.

❋ *"Minimum initial failure strength"* typically determined by conventional stress analysis methods used in commercial airplane design for insuring that minimum strength will always exceed regulatory requirement.

⌖ *"Estimated maximum initial failure strength"* typically determined from large finite element models capable of load redistribution in plastic range. Initial failure determined by input % strain at failure.

- *Separate analysis* of deformations of spanwise beam #1 maintenance access doors indicates that a pressure gradient (aft) of 45-55 psi was probably present at the left door and a gradient of 20 -25 psi at the right door.